

Two sub-band conductivity of Si quantum well

M. Prunnila* and J. Ahopelto

VTT Information Technology, P.O.Box 1208, FIN-02044 VTT, Espoo, Finland

We report on two sub-band transport in double gate SiO₂-Si-SiO₂ quantum well with 14 nm thick Si layer at 270 mK. At symmetric well potential the experimental sub-band spacing changes monotonically from 2.3 to 0.3 meV when the total electron density is adjusted by gate voltages between $\sim 0.7 \times 10^{16} - 3.0 \times 10^{16} \text{ m}^{-2}$. The conductivity is mapped in large gate bias window and it shows strong non-monotonic features. At symmetric well potential and high density these features are addressed to sub-band wave function delocalization in the quantization direction and to different disorder of the top and bottom interfaces of the Si well. Close to bi-layer/second sub-band threshold the non-monotonic behavior is interpreted to arise from scattering from localized band tail electrons.

PACS numbers: 73.40.-c, 72.20.-i

Keywords: two-dimensional electron gas, localization, resonant coupling, bi-layer, silicon

1. INTRODUCTION

Development of silicon-on-insulator technology has enabled fabrication of silicon heterostructure devices where thin single crystalline Si film is sandwiched between amorphous SiO₂ layers. This kind of SiO₂-Si-SiO₂ quantum well provides a unique material system where electron density can be tuned in a broad range due to high potential barriers formed by the SiO₂ layers. Previous work on SiO₂-Si-SiO₂ quantum wells has mainly focused on single and bi-layer magneto transport [1, 2, 3]. In this work we focus on the issue how the two sub-band or bi-layer transport affects the low temperature conductivity of double gate SiO₂-Si-SiO₂ quantum well with 14 nm thick Si layer.

2. EXPERIMENTAL

The samples were fabricated on commercially available (100) silicon-on-insulator wafer as described in detail in Ref. [3]. The cross-sectional sample structure consist of n⁺ Si top gate, top gate oxide (OX), Si well, back gate oxide (BOX) and n⁺ Si back gate. The top gate is polycrystalline while the back gate is crystalline silicon. All results reported here were obtained from a 100 μm wide Hall bar sample with 400 μm voltage probe distance. The layer thickness for the Si well, top gate oxide and back gate oxide were $t_w = 14 \text{ nm}$, $t_{\text{OX}} = 40 \text{ nm}$, and $t_{\text{BOX}} = 83 \text{ nm}$, respectively. Figure 1 shows the schematic device cross-section together with self-consistent wave functions and effective potential at two total electron density (n) values.

In the experiments the sample was mounted to a sample holder of a He-3 cryostat, which was at base temperature (270 mK). The electron density was determined

from the Shubnikov- de Haas (SdH) oscillations of the diagonal resistivity ρ_{xx} utilizing the standard methods: in the single sub-band gate bias windows ρ_{xx} was measured as a function of the gate voltages at constant magnetic field B and n was determined from the minimum positions of ρ_{xx} . In the presence of two sub-bands ρ_{xx} was recorded as a function of B . Then a Fourier transform was performed numerically to $\rho_{xx}(1/B)$ and a peak position multiplied by e/h (e fundamental charge, h Plank's constant) in the spectrum gave the sheet density per degeneracy of a sub-band.

3. RESULTS AND DISCUSSION

3.1. Sub-band densities at balanced gate bias

Left vertical axis of Fig. 2 shows the different electron densities as a function of top gate voltage V_{TG} along the balanced (or symmetric) gate bias line where the back gate voltage $V_{\text{BG}} = V_{\text{TG}}t_{\text{BOX}}/t_{\text{OX}}$. This choice of

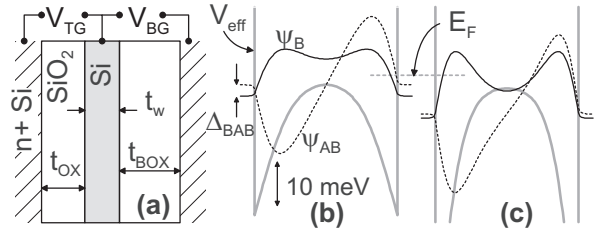


FIG. 1: (a) Schematic cross-section of the sample and gate biasing in the experiments. The dimensions are $t_w = 14 \text{ nm}$, $t_{\text{OX}} = 40 \text{ nm}$ and $t_{\text{BOX}} = 83 \text{ nm}$. (b)&(c) Self-consistent bonding and anti-bonding electron wave functions together with the effective potential V_{eff} in the 14 nm thick Si well at balanced gate bias within the Hartree approximation. The wave functions are offsetted so that $\Psi_{\text{B,AB}} = 0$ is equal to the corresponding eigen energy $E_{\text{B,AB}}$. (b): $n = 1.0 \times 10^{16} \text{ m}^{-2}$. (c): $n = 2.8 \times 10^{16} \text{ m}^{-2}$.

*Corresponding author
email: mika.prunnila@vtt.fi

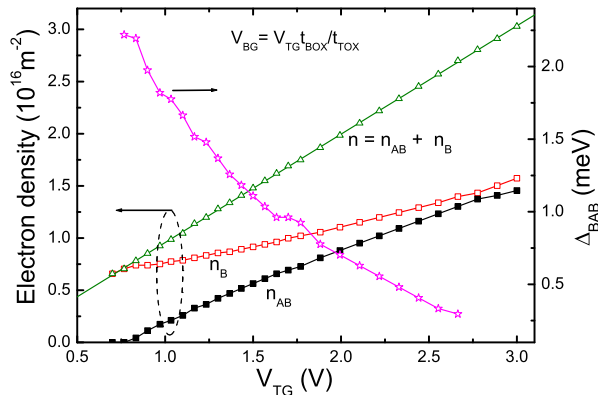


FIG. 2: Right axis: total electron density (n) and sub-band densities (n_B, n_{AB}) as a function of top gate voltage along the balanced gate line of a 14 nm thick Si well. The densities are determined from SdH oscillations at 270 mK. Left axis: Sub-band energy spacing calculated from n_B and n_{AB} assuming ideal 2D density of states.

gate biases produce symmetric potential in the Si well. The total density n is obtained by summing the bonding sub-band n_B and anti-bonding sub-band densities n_{AB} . On the balanced gate line the threshold for n_{AB} is at $V_{TG} \approx 0.8$ V and $n = n_B \approx 0.7 \times 10^{16} \text{ m}^{-2}$. Note that the SdH method does not reveal the degeneracies of the system. We have made an assumption that both sub-bands arise from the high perpendicular mass valleys (non-primed valleys), which gives the total degeneracy of four after including the spin degeneracy. Our *a priori* assumption is validated by noting that V_{TG} vs. $n = n_B + n_{AB}$ slope corresponds accurately to the total gate capacitance. The light perpendicular mass valleys (non-primed valleys) have a total degeneracy of eight and this degeneracy would lead to incorrect total density.

Right vertical axis of Fig. 2 shows the bonding anti-bonding energy gap Δ_{BAB} which is obtained from n_B and n_{AB} by assuming ideal 2D density of states together with bulk effective mass $m^* = m_t = 0.19m_0$ parallel to the quantum well plane. The increased gate drive and n leads to expected reduction of Δ_{BAB} due to the potential barrier formation in the middle of the Si well as demonstrated by the self-consistent calculations in Figs. 1(b) and (c). The calculated Δ_{BAB} is larger than the experimental one by ~ 0.72 meV (on average) in the density range of Fig. 2 (not shown). This discrepancy can be explained by noting that we have neglected the exchange and correlation effects in the calculations.

3.2. Conductivity and mobility

Figure 3(a) shows (zero magnetic field) conductivity $\sigma = 1/\rho_{xx}$ measured as a function of top and back gate voltages [4]. The scales of the voltage axes in Fig. 3(a)

are chosen in such a manner that if we move perpendicularly to the balanced bias line the electron density stays (roughly) constant, i.e., we move along $n = \text{const.}$ line and merely shift the position of the electron gas inside the Si slab. In the gate bias regions $V_{TG} \lesssim 0$ or $V_{BG} \lesssim 0$ only single sub-band is occupied and σ behaves monotonically, which is expected on the basis of simple Coulomb - surface roughness scattering picture and is consistent with mobility measurements of sub-10 nm thick Si well [3].

The overall asymmetry of the conductivity with respect to the symmetric bias line arises from the different quality of the top (Si-OX) and back (Si-BOX) interfaces of the Si well. The back interface has substantially larger disorder in comparison to the top interface as can be observed from Figs. 3(b) and (c), which show the back interface and top interface mobilities $\mu = \sigma/en$, i.e., the mobilities along the axes of Fig. 3(a). Note that the n -axis of Figs. 3(b) and (c), together with n plotted in Fig. 2, also give an idea of the magnitude of electron density. The observed disorder difference is mainly due to larger surface roughness of the Si-BOX interface [3] consistent with the fact that the top-back mobility ratio actually increases as a function of carrier density. At low density surface roughness plays a minor role and the mobilities almost coincide, which is also partly due to electron wave function spreading throughout the Si well. The presence of the two Si-SiO₂ interfaces also reduce the peak mobility and shift it towards higher electron densities [5].

In the bias window $V_{TG, BG} \gtrsim 0$ the conductivity behaves strongly non-monotonically. We can observe, e.g., that close to threshold $\sigma(V_{TG}, V_{BG})|_{n=\text{const.}}$ has a local minimum at symmetric bias. Note that at symmetric bias the second sub-band starts to populate at $V_{TG} \approx 0.8$ V (as was shown in the previous Sub-section) and the minimum is particularly strong when we are below this threshold. If we increase the gate biases the minimum at $V_{BG} = V_{TG} t_{BOX}/t_{OX}$ for $\sigma(V_{TG}, V_{BG})|_{n=\text{const.}}$ is clearly splitted into two local minima, which follow closely the axes of the Figure. The minimum that follows V_{TG} -axis is illustrated more clearly in Fig. 4 which shows $\sigma(V_{BG}, V_{TG}=\text{const.})$. Note that if we would plot $\sigma(V_{TG}, V_{BG}=\text{const.})$ we would obtain a similar curve (only the magnitude of σ would be different due to different quality of the Si-OX and Si-BOX interfaces). By comparing the high magnetic field ρ_{xx} data of Ref. [3] and Fig. 3(a) we note that the local minimum in the vicinity of $V_{BG, TG} \sim 0$ for $\sigma(V_{BG, TG}, V_{TG, BG}=\text{const.})$ occurs at the position which is the threshold where ρ_{xx} starts to show signatures of bi-layer transport.

The above non-monotonic behavior of σ has a striking similarity to the substrate bias experiments of bulk Si inversion layers, where it was found that a positive substrate bias tends to reduce the mobility [6]. This effect has been addressed to spin flip scattering from singly populated localized band tail states of higher sub-bands[7] (, whose population increases with substrate bias in bulk

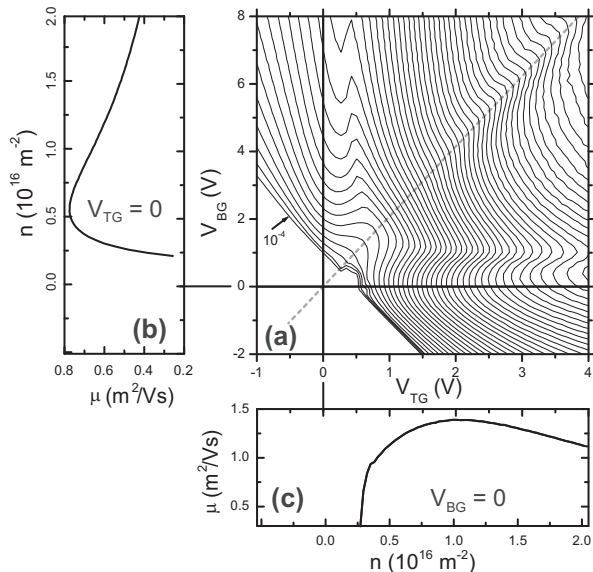


FIG. 3: (a) Contour plot of conductivity σ measured at 270 mK. The contour spacing is 10^{-4} $1/\Omega$. The dashed line is the balanced gate line $V_{BG} = V_{TG}t_{BOX}/t_{OX}$. (b) Back interface mobility as a function of V_{BG} (right vertical axis) and n (left vertical axis). (c) Top interface mobility as a function of V_{TG} and n .

devices). Scattering from localized band tail electrons is the most probable origin for the behavior of σ in the vicinity of the $V_{TG(BG)} \sim 0$ at high $V_{BG(TG)}$ and around $V_{BG} = V_{TG}t_{BOX}/t_{OX}$ below the threshold of the second sub-band. In detail, e.g., for the data in Fig. 4: the conductivity saturates and starts to decrease because the population in the localized band tail of the second sub-band increases and these localized electrons scatter the electrons in the mobile first sub-band. Then at certain threshold the Fermi level passes through "the mobility edge" of the second sub-band and the conductivity starts to increase due to presence of two sub-bands with extended states.

If we increase the electron density by gate bias beyond the threshold of the second sub-band the local minimum in $\sigma(V_{BG}, V_{TG})|_{n=\text{const.}}$ at $V_{BG} = V_{TG}t_{BOX}/t_{OX}$ disappears due to presence of (solely) extended states. Then above $V_{TG} \sim 2$ V another minimum appears. This is indicated by the down arrows in Fig. 4. The origin of this feature is related to the resonance effect observed in tunneling coupled double quantum wells (often referred as resistance resonance) [8, 9, 10]. At high electron density and gate bias (at both gates) the double sub-band system in the Si well can be described equivalently as a weak or medium coupling bi-layer, which is a direct consequence of the barrier formation in the middle of the well [see Figs. 1(b)&(c)]. Far away from the balanced gate bias $V_{BG} = V_{TG}t_{BOX}/t_{OX}$ the barrier localizes the wave functions of the different layers or

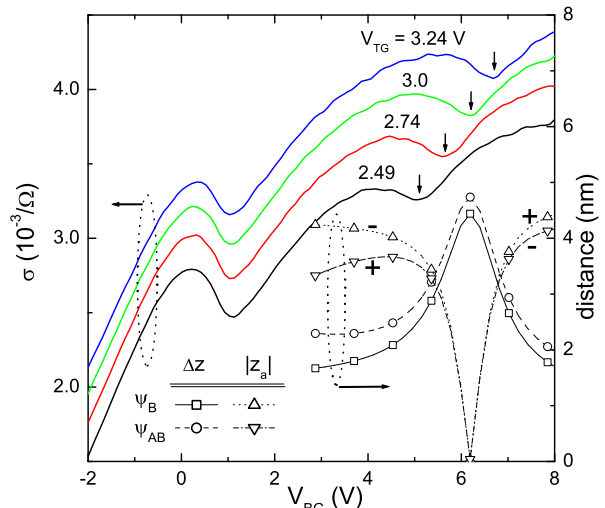


FIG. 4: Left axis: conductivity as a function of back gate voltage. \downarrow indicate $V_{BG} = V_{TG}t_{BOX}/t_{OX}$. Right axis: deviation (position uncertainty) Δz and absolute value of average position z_a of the sub-band wave functions. The zero is in the middle of the well and \pm indicate the sign of z_a . The calculation corresponds to the $V_{TG} = 3.0$ V curve.

sub-bands to the different sides of the well. At balanced gate bias the sub-band wave functions delocalize across the well. This localization - delocalization is illustrated in Fig. 4 (right axis) where we show the average position $z_a = \langle z \rangle = \langle \Psi | z | \Psi \rangle$ ($\Psi = \Psi_{B,AB}$) and deviation (position uncertainty) $\Delta z = \sqrt{\langle z^2 \rangle - \langle z \rangle^2}$ of the sub-bands. At balanced bias Δz has a maximum and $z_a = 0$, which results in mobility reduction of the sub-band that otherwise is localized in the vicinity of the less disordered interface while the mobility of the other sub-band stays practically unaffected [9]. This leads to the local minimum in σ at $V_{BG} = V_{TG}t_{BOX}/t_{OX}$ at high electron densities. The detailed form of this minimum is strongly affected by the momentum relaxation time and quantum lifetime [10] and further discussion will be published elsewhere.

4. SUMMARY

We have reported on two sub-band transport in 14 nm thick Si quantum well at 270 mK. The conductivity of the quantum well showed non-monotonic double gate bias dependency. At symmetric well potential and high density these were addressed to sub-band wave function delocalization in the quantization direction and to different disorder of the top and bottom interfaces of the Si well. In the gate bias regimes close to 2nd sub-band / bi-layer threshold the non-monotonic behavior was interpreted to arise from spin flip scattering from singly populated localized band tail states of higher sub-bands.

Acknowledgments

financial support through project # 205467.

M. Markkanen is thanked for assistance in the sample fabrication. Academy of Finland is acknowledged for

-
- [1] K. Takashina, A. Fujiwara, S. Horiguchi, Y. Takahashi, and Y. Hirayama, *Phys. Rev. B* **69**, 161304(R) (2004).
 - [2] M. Prunnila, J. Ahopelto, and H. Sakaki, *Phys. Stat. Sol.(a)* **202**, 970 (2005).
 - [3] M. Prunnila, J. Ahopelto, and F. Gamiz, *Solid State Electronics*, in print, also available at <http://lanl.arxiv.org/cond-mat/0506073> (2005).
 - [4] The obscured behavior of the σ contours in the vicinity of the threshold and below the symmetric bias line is an experimental artefact explained in [3].
 - [5] M. Prunnila, J. Ahopelto, and F. Gamiz, *Appl. Phys. Lett.* **84**, 2298 (2004).
 - [6] A. B. Fowler, *Phys. Rev. Lett.* **34**, 15 (1975).
 - [7] X. G. Feng, D. Popovic, and S. Washburn, *Phys. Rev. Lett.* **83**, 368 (1999).
 - [8] A. Palevski, F. Beltram, F. Capasso, L. Pfeiffer, and K. W. West, *Phys. Rev. Lett.* **65**, 1929 (1990).
 - [9] Y. Ohno, M. Tsuchiya, and H. Sakaki, *Appl. Phys. Lett.* **62**, 1952 (1993).
 - [10] Y. Berk, A. Kamenev, A. Palevski, L. N. Pfeiffer, and K. W. West, *Phys. Rev. B* **50**, 15420 (1994).